

Photoinduced Desorption of Xe from Porous Si following Ultraviolet Irradiation: Evidence for a Selective and Highly Effective Optical Activity

Gil Tokor and Micha Asscher*

Institute of Chemistry, The Hebrew University of Jerusalem, Jerusalem, 91904, Israel

(Received 20 April 2011; revised manuscript received 5 July 2011; published 11 October 2011)

Photoinduced desorption (PID) of Xe from porous silicon (PSi) following UV irradiation has been studied. A nonthermal, morphology, and wavelength dependent phenomenon with more than 3 orders of magnitude enhancement of Xe PID within pores over atoms adsorbed on top of flat surfaces has been recorded, displaying extraordinary large cross sections up to $\sigma_{\text{Xe/PSi}} = 2 \times 10^{-15} \text{ cm}^2$. A long-lived, photoinduced, charge separated silicon-xenon complex is proposed as the precursor for this remarkable photodesorption process.

DOI: 10.1103/PhysRevLett.107.167402

PACS numbers: 78.66.Jg, 68.43.Tj, 82.50.Hp, 82.65.+r

Photochemistry on surfaces is important for a fundamental scientific understanding of light-matter interactions and is motivated mainly by applications such as photolithography, photovoltaics, and photocatalysis [1,2]. Photodissociation of N_2O on Si (100) has been studied [3] as a mild silicon oxidation process with cross sections $\sigma_{\text{Si}} = 4 - 5 \times 10^{-18} \text{ cm}^2$ for irradiation at 193 nm. Similar cross sections were found for photodesorption of disilane from deuterium covered Si(100) [4]. Photoinduced desorption (PID) of Xe from flat Si(100) is significantly less efficient with cross sections of $3 \times 10^{-20} \text{ cm}^2$ and $1.2 \times 10^{-20} \text{ cm}^2$ for 351 and 532 nm irradiation, respectively [5]. A similar process on O covered Si revealed higher cross sections ($5 \times 10^{-18} \text{ cm}^2$ for 351 nm irradiation) and wavelength dependence [6]. Atomic and molecular PID often involve hot electron attachment leading to evolution and spatial nuclei separation on a repulsive excited potential energy surface (PES) that results in desorption via the Menzel-Gomer-Redhead (MGR) mechanism [1–3,7]. An alternative PID model involves a decay from an attractive charge separated excited PES to the repulsive part of the ground state. This one is based on a mechanism proposed by Antoniewicz [8].

In the case of Xe PID from flat metals and semiconductors, no affinity levels are available to support desorptive electron attachment (DEA); therefore, the standard MGR model cannot be applied to explain PID and indeed the reported cross sections for Xe PID from such smooth surfaces are relatively small [5].

Porous silicon (PSi) has been extensively studied [9] since the discovery of its photoluminescence [10]. Freshly prepared PSi samples are passivated by hydrogen atoms, having complex and ramified inner surfaces with a large surface area, up to 500 cm^2 per gram [11,12]. Adsorption and thermal desorption kinetics of Xe from smooth and PSi surfaces were recently reported [13].

Here we report on the observation of a selective and remarkably efficient photoinduced desorption (PID) of Xe from porous silicon under UV irradiation. It was found that

internal morphology and size of the pores and the excitation wavelength strongly affect the overall photoresponse of this system.

Two types of PSi samples were examined, characterized by a different degree of inner roughness and porosity: mesoporous and nanoporous silicon. The preparation of mesoporous samples is based on electrochemical etching current density of 50 mA/cm^2 in a solution of 6% HF (aqueous 48 wt %) with 8 mM KMnO_4 , as previously described [14]. Nanoporous samples were fabricated by chemical etching (stain etching [15]) in a solution containing 0.5 M FeCl_3 , 80% (vol) $\text{HF}_{(\text{aq})}$, and 20% (vol) H_2SO_4 (95–97 wt %) for 30 min. As a reference, flat and smooth Si-H surfaces were obtained by exposing a native $\text{SiO}_2/\text{Si}(100)$ sample to concentrated HF solution for 2 min.

The samples were subsequently attached to the bottom of a closed cycle refrigerator within a UHV chamber (base pressure $\sim 5 \times 10^{-10}$ Torr) with Auger spectrometer and cooling capability down to $40 \pm 2 \text{ K}$. A retractable quadrupole mass spectrometer was employed for selective temperature programmed desorption (TPD) measurements from the illuminated part of the sample (see Fig. 1) and for real time detection of photodesorbing species. Low power excimer laser operating at 193 nm (ArF) and 248 nm (KrF) and the 3rd and 4th harmonic of Nd-YAG laser were the UV light sources. Maximal laser powers at the sample surface were 1.2 mJ/pulse (193 nm), 0.5 mJ/pulse (248 nm), 16 mJ/pulse (266 nm), and 12 mJ/pulse (355 nm) with an equal beam footprint on the sample of $\sim 0.5 \text{ cm}^2$.

Following the UHV-PID studies (see below), samples morphology was *ex situ* characterized by high resolution scanning electron microscope (HR-SEM). The top views of the mesoporous [3.7 μm deep pores, $50 \pm 20 \text{ nm}$ in diameter Fig. 2(a)] and nanoporous [1.5 μm deep with average pore diameter $< 10 \text{ nm}$, Fig. 2(b)] are shown as insets in Fig. 2.

TPD measurements following UV laser irradiation were employed to quantify the efficiency and selectivity of the

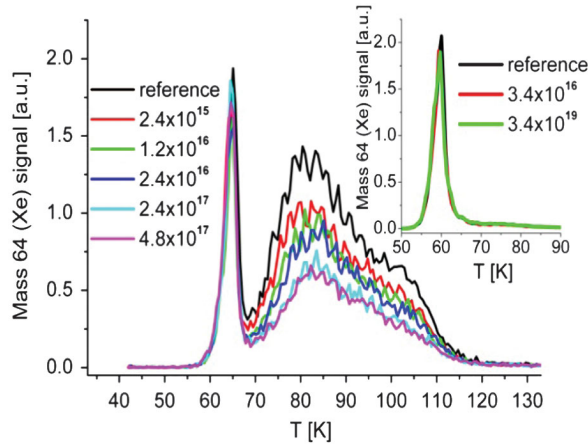


FIG. 1 (color). Postirradiation TPD of 2.5 ML Xe ($m/z = 64$) on flat (inset) and mesoporous silicon samples, at the indicated exposures to 193 nm photons. The porous sample consists of 50 nm wide pores, 3.7 μm deep, with a heating rate of 5 K/sec.

PID process of Xe from flat and porous silicon samples. Figure 1 displays TPD spectra from a mesoporous silicon sample and from a smooth hydrogen terminated silicon surface (Fig. 1, inset) following irradiation at 193 nm. An upper limit cross section for PID of $5 \pm 3 \times 10^{-20} \text{ cm}^2$ has been determined for the smooth, nonporous Si(100)-H sample from the decay of the area under the single Xe desorption peak at 60 K following prolonged exposure to the UV light, consistent with previous studies [5]. The two distinct Xe desorption peaks in Fig. 1 at 65 K (narrow, low temperature—LT) and 85 K (broad, high temperature—HT) are attributed to adsorbates on the top surface and in pore's internal surfaces, respectively [13]. The LT peak is practically unaffected by the 193 nm irradiation, as was the response over the flat surface (Fig. 1, inset). In contrast, the HT peak exhibits very different behavior: a single laser pulse (2.4×10^{15} photons/ cm^2 , 193 nm) depletes a significant portion ($\sim 15\%$) of the adsorbed population at the inner pores. The relatively large fraction of photoactive population, undergoing PID ($\sim 50\%$ of the HT peak photo-desorbed as a result of exposure to 2×10^{17} photons/ cm^2 at 193 nm) suggests that at the adsorption temperature (40 K) the sample is not homogeneously covered by adsorbates. Since the extinction coefficient of PSi is $2 \times 10^5 \text{ cm}^{-1}$ (193 nm) and $4 \times 10^5 \text{ cm}^{-1}$ (for both 248 and 266 nm) [16], light absorbance occurs at the top hundred nanometers. Our samples were several microns deep; therefore, significant depletion suggests that a large fraction of the adsorbates occupies this photoactive layer at the adsorption temperature (40 K).

In Fig. 2 the integrated area under the remaining HT peak is plotted as a function of an accumulated number of photons for the two samples—mesoporous and nanoporous silicon. In both experiments two photochemically active populations were identified that differ in their photoresponse. The mesoporous sample [Fig. 2(a)] is

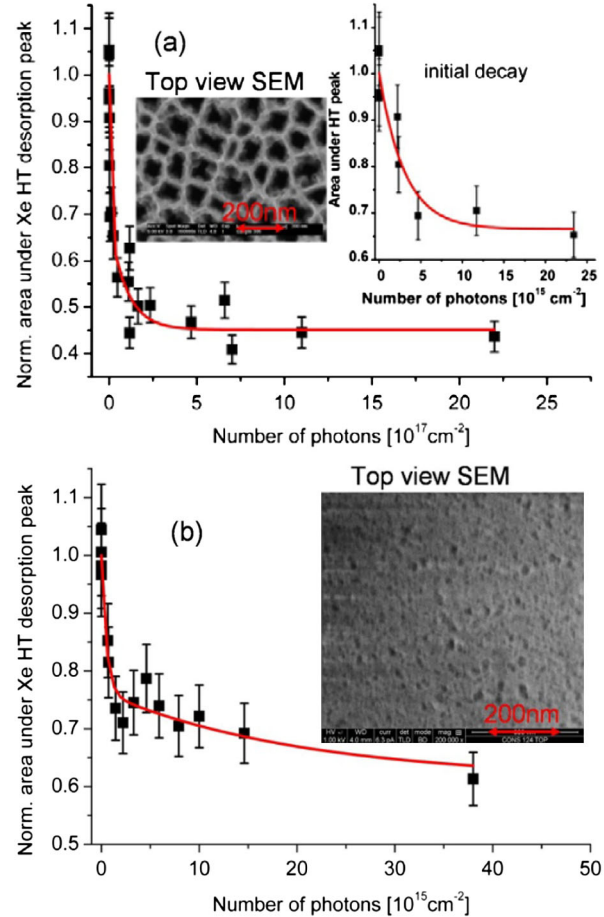


FIG. 2 (color online). Integrated area under Xe high temperature (HT) desorption peak (85 K) from (a) meso- and (b) nano-PSi vs the number of photons at $\lambda = 193 \text{ nm}$. Xe coverage was 2.5 ML equivalent and the PSi layers were 3.7 and 1.5 μm deep for the meso and nano samples, respectively. Insets: top view SEM images (the distance bar is 200 nm in both images). (a) inset: zoom-in on the fast initial population depletion of the meso-PSi sample. Note the different scales of the number of photons in (a) (10^{17}) and in the inset of (a) and in (b) (10^{15}).

characterized by PID cross sections of $3 \times 10^{-16} \text{ cm}^2$ [32%, (HT) fast] and $0.1 \times 10^{-16} \text{ cm}^2$ [24%, (HT) slow] when irradiated at 193 nm. Similar results for 248 nm (not shown) were $0.7 \times 10^{-16} \text{ cm}^2$ [20%, (HT) fast] and $0.03 \times 10^{-16} \text{ cm}^2$ [25%, (HT) slow]. Xe-PID on top of the nanoporous, stain etched sample [Fig. 2(b)] had higher cross sections of $20 \times 10^{-16} \text{ cm}^2$ [25%, (HT) fast] and $0.5 \times 10^{-16} \text{ cm}^2$ [15%, (HT) slow] at 193 nm and $10 \times 10^{-16} \text{ cm}^2$ [35%, (HT) fast] and $0.3 \times 10^{-16} \text{ cm}^2$ [18%, (HT) slow] at 248 nm (not shown).

The most photoresponsive population (fast) in the nanoporous sample decays within 1–2 laser pulses, leading to some uncertainties in cross sections obtained from the TPD of remaining Xe population.

In order to better isolate the fast decaying photoresponsive population, real time PID tracking experiments of the

actually photodesorbing atoms in each laser pulse were performed, as depicted for mesoporous [Fig. 3(a)] and nanoporous [Fig. 3(b)] samples, irradiated at 193 nm.

The amplitude of the first laser pulse-PID peak (for 193 nm irradiation) was found to be nonlinear with respect to the laser fluence [Fig. 3(a), inset], responding in a power law relation of $Y(\text{PID}) = AI_{\text{in}}^{1.7 \pm 0.3}$ with $Y(\text{PID})$ being the PID yield, I_{in} the incident laser fluence, and A a constant.

In addition, the PID process was found sensitive to excitation wavelength, becoming less efficient with reduced photon energy [Fig. 3(b), inset]. Most of the PID signal decays following the first pulse at 193 nm even at the lowest fluence (0.45 mJ/cm^2), suggesting that the cross sections reported here for the most active population are only lower limits.

This remarkably efficient and selective PID (more than 3 orders of magnitude larger than on flat Si surfaces, the largest PID cross section from solid substrates reported so far, to the best of our knowledge) differs from other

photoinduced phenomena observed on flat surfaces [1–6]. It suggests a unique energy conversion mechanism from photons to adsorbates occupying inner pore walls that are corrugated and filled with nanotips. A possible PID mechanism is discussed below.

In spite of the low laser power used in our work, laser induced thermal desorption has to be considered as a possible, indirect PID route. Since readsorption is significantly more important and probable in the inner pores, thermal desorption should have resulted in more efficient desorption from the top surfaces (LT).

The PID cross sections reported here for P*Si* were found to be wavelength dependent while the absorption coefficients of P*Si* at the UV wavelengths used in our experiments, 193, 248, and 266 nm, are practically identical [16] (all three photon energies are above the work function of the flat, H-terminated silicon—4.6 eV [17]). Moreover, at 266 nm, 5 times higher laser fluence was employed, without any measurable effect on the depletion of the LT Xe population. The power dependence observed is significantly weaker than the power law dependence expected for thermally induced processes, predicting an exponential dependence on peak temperature, resulting in a power law of $Y(\text{PID}) = AI_{\text{in}}^{4 \pm 1}$.

Based on these observations, we conclude that the Xe-PID process reported here is a nonthermal one, at the excitation wavelengths below 250 nm.

Several mechanisms for PID were discussed in the literature: desorption induced by electron-hole recombination associated with energy transfer to surface phonons was the mechanism proposed for Xe desorption from clean and deuterated Si (100) [5,6]. This mechanism leads to cross sections that are wavelength independent and cannot explain the PID selectivity observed here.

Pauli repulsion of collectively oscillating electrons (plasmons) was used to explain hyperthermal PID of Xe from Ag nanoparticles [18]. No plasmons, however, are known to be excitable in the case of porous silicon at the photon energies employed in our study.

Preliminary experiments we have conducted where low energy electrons (5–20 eV) were used in order to stimulate desorption (ESD) on flat and porous silicon surfaces (not shown) revealed that no Xe desorption was detectable. This indicates ESD cross section for Xe of significantly less than $0.03 \times 10^{-16} \text{ cm}^2$. Although the penetration depth of electrons at this energy range, estimated from their mean free path values, is limited to only 3–5 nm, Xe atoms at the top surface are fully exposed, yet nonresponding to these low energy electrons. Typical ESD cross sections of molecular adsorbates are at the 10^{-15} cm^2 range [19]. The difference between ESD and PID in our system is the photogenerated, localized, and long-lived holes within the porous substrate and the sensitivity of PID to the substrate level of porosity. These holes are believed to be stabilized at nanotips where photogenerated electrons are

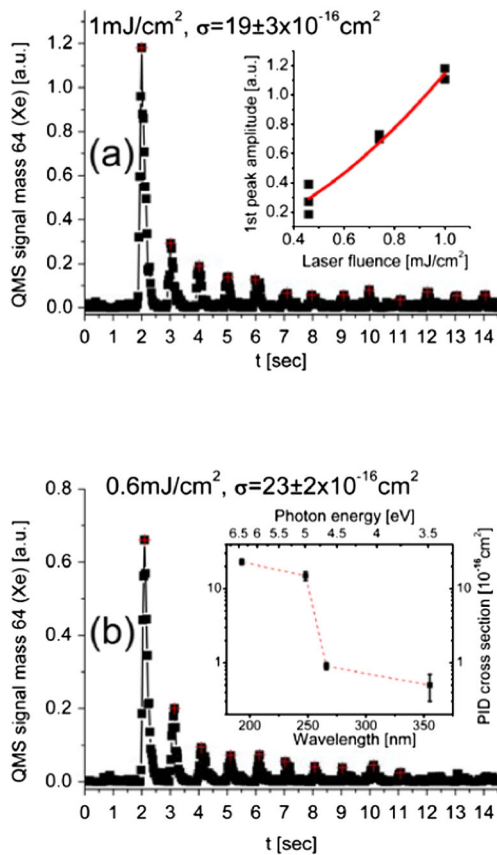


FIG. 3 (color online). Real-time tracking of Xe PID from (a) meso- and (b) nano-P*Si*. Xe coverage was 2.5 ML equivalent, QMS signal at mass 64 measured during single pulsed lasing (1 Hz, 193 nm at the relevant laser energy per pulse). The insets contain (a) fluence dependence of first peak amplitude for the meso-P*Si* and (b) wavelength dependence of PID cross section for the nano-P*Si*. Exponential decay through maxima of the PID signal was used for PID cross section derivation (not shown).

preferentially emitted because of the particularly low work function expected at these sites.

Low energy photoelectron attachment to Xe clusters [20] may lead to the formation of long-lived, charge separated $[\text{Si}_{ip}^+ - \text{Xe}_n^-]$ complexes. We cannot rule out an alternative mechanism based on the Auger process where an electron from the highest Xe occupied ground electronic state decays and neutralizes the hole located on the silicon tip. This mechanism results in a positively charged, adsorbed Xe^+ that is attracted inward to the surface via an Antoniewicz-like mechanism [8,21]. Such a process, however, is less likely to dominate for the current system. Long-lived, negatively charged xenon clusters as a precursor for Xe-PID from oxidized silicon was proposed to explain the behavior of the majority population, as determined by time-of-flight measurements [6], and we conclude it should be the dominant mechanism to explain our results as well.

The eventual $e-h$ recombination after a critical, prolonged residence time (τ_c) at the excited PES leads to the repulsive part of the ground state, resulting in desorption. In our case, the low mobility values of holes in PSi at the operating surface temperature [22] and the relatively stable negatively charged Xe_n^- clusters, with n being approximately in the range $1 < n < 3$ are thought to be responsible for the extended lifetime of the excited, charge separated, $\text{PSi}_{ip}^+ - \text{Xe}_n^-$ complex. This prolonged lifetime should lead to a significant increase in desorption probability [1,2]. The proposed mechanism is consistent with the observed selectivity of the PID process, since the top surface is relatively flat compared to inner pore surfaces. Field emission studies have demonstrated that electron emission from corrugated PSi tips is indeed enhanced by an order of magnitude compared to noncorrugated ones [23]. We consider this as supporting evidence for our hypothesis of preferential photoexcitation and photoelectron emission from corrugated tips, because of their lower work function than on flat surfaces. The tenfold decrease in PID cross section with decreasing photon energy [Fig. 3(b), inset] from 5 to 4.66 eV can be explained by a smaller photoelectron emission probability when the photon energy decreases towards (and below) the work function.

In conclusion, We have shown that photoinduced desorption of Xe from internal surfaces of porous silicon is more efficient by 3 to 4 orders of magnitude compared to similar processes on flat solid surfaces [1–6]. The large photoactive population implies high density of adsorbates at the top 100 nm section of the PSi samples. A density gradient of this kind apparently arises from limited diffusion at the adsorption temperature (40 K). The wavelength and morphology dependence of the PID process suggests that PID from PSi can be explained by an Antoniewicz-like mechanism: a trapped photohole induces partial charge

transfer to xenon atoms that form negatively charged clusters, stabilizing a long-lived, charge separated exciton. Its decay leads to repulsive interactions, leading to enhanced desorption probability. These results suggest that photocatalytic and photovoltaic processes within PSi matrix may potentially lead to unusually efficient systems.

This research was partially supported by the Israel Science Foundation and the U.S.-Israel Binational Science Foundation. Support from A. Sa'ar and his co-workers concerning PSi preparation procedures is acknowledged.

*Corresponding author.

asscher@chem.ch.huji.ac.il

- [1] X.-L. Zhou, X.-Y. Zhu, and J.M. White, *Surf. Sci. Rep.* **13**, 73 (1991).
- [2] *Laser Spectroscopy and Photochemistry on Metal Surfaces, Parts I and II*, edited by H. -L. Dai and W. Ho (World Scientific, New York, 1995).
- [3] H. Kato, J. Lee, K. Sawabe, and Y. Matsumoto, *Surf. Sci.* **445**, 209 (2000).
- [4] S. Wright and E. Hasselbrink, *J. Chem. Phys.* **114**, 7228 (2001).
- [5] K. Watanabe, H. Kato, and Y. Matsumoto, *Surf. Sci.* **446**, L134 (2000).
- [6] K. Watanabe and Y. Matsumoto, *J. Chem. Phys.* **115**, 4259 (2001).
- [7] D. Menzel and R.J. Gomer, *J. Chem. Phys.* **41**, 3311 (1964).
- [8] P.R. Antoniewicz, *Phys. Rev. B* **21**, 3811 (1980).
- [9] A. G. Cullis, L. T. Canham, and P.D.J. Calcott, *J. Appl. Phys.* **82**, 909 (1997).
- [10] L. T. Canham, *Appl. Phys. Lett.* **57**, 1046 (1990).
- [11] D. Kovalev *et al.*, *Phys. Rev. Lett.* **87**, 68 301 (2001).
- [12] D.B. Mawhinney, J.A. Glass, Jr., and J.T. Yates, Jr., *J. Phys. Chem. B* **101**, 1202 (1997).
- [13] A. Paldor, G. Toker, Y. Lilach, and M. Asscher, *Phys. Chem. Chem. Phys.* **12**, 6774 (2010).
- [14] Y.H. Ogata *et al.*, *Electrochemistry* **75**, 270 (2007).
- [15] M. Nahidi and K. W. Kolasinski, *J. Electrochem. Soc.* **153**, C19 (2006).
- [16] F. De Fillippo *et al.*, *Phys. Status Solidi (a)* **182**, 261 (2000).
- [17] A. Y. Anagaw, R. A. Wolkow, and G. A. DiLabio, *J. Phys. Chem. C* **112**, 3780 (2008).
- [18] K. Watanabe, K.H. Kim, D. Menzel, and H.J. Freund, *Phys. Rev. Lett.* **99**, 225501 (2007).
- [19] Y. Lilach and M. Asscher, *J. Phys. Chem. B* **108**, 4358 (2004).
- [20] H. Haberland, T. Kolar, and T. Reiners, *Phys. Rev. Lett.* **63**, 1219 (1989).
- [21] A. Abe and K. Yamashita, *Chem. Phys. Lett.* **343**, 143 (2001).
- [22] P. A. Forsh *et al.*, *J. Exp. Theor. Phys.* **107**, 1022 (2008).
- [23] M. Takai *et al.*, *Appl. Phys. Lett.* **66**, 422 (1995).